A cloud line over the Gulf Stream

Xiaofeng Li,[1] Weizhong Zheng,[2] William G. Pichel,[1] Cheng-Zhi Zou,[1]
Pablo Clemente-Colón,[1] and Karen S. Friedman[1]

Received 4 March 2004; revised 7 April 2004; accepted 17 April 2004; published 28 July 2004.

[1] A 1000 km long cloud-line over the major axis of the Gulf Stream was detected in imagery from a number of satellites on April 24, 2001. Analysis of environmental conditions shows that such a cloud-line is formed when the synoptic low-level wind is parallel to the Gulf Stream axis and the sky is clear, conditions that rarely occur in the high-temperature and high-moisture Gulf Stream region. The PSU-NCAR fifth-generation Mesoscale Model (MM5) is used to study the cloud line. Results show that upward motion of the air in the middle of the Gulf Stream, caused by mesoscale solenoidal circulation induced by the large surface thermal gradient, is the source for the large cloud-line formation. This cloud-line formation mechanism is different from that of commonly observed ship cloud lines induced by ship-stack emissions, and its extent is much longer than that of cloud lines induced by lake effects. *INDEX TERMS:* 3307 Meteorology and Atmospheric Dynamics: Boundary layer processes; 3329 Meteorology and Atmospheric Dynamics: Mesoscale meteorology; 3339 Meteorology and Atmospheric Dynamics: Ocean/atmosphere interactions (0312, 4504); 3360 Meteorology and Atmospheric Dynamics: Remote sensing. **Citation:** Li, X., W. Zheng, W. G. Pichel, C.-Z. Zou, P. Clemente-Colón, and K. S. Friedman (2004), A cloud line over the Gulf Stream, *Geophys. Res. Lett.*, *31*, L14108, doi:10.1029/2004GL019892.

1. Introduction

[2] Satellite observations have shown that smoke particles emitted from a ship may induce the formation of a ship-track cloud line in a cloudless sky or change existing cloud structures [*Coakley et al.*, 1987; *Rakde et al.*, 1989]. Another cloud-line formation mechanism can be attributed to low-level baroclinicity in the atmospheric boundary layer induced by the surface thermal gradient of the Earth [*Holton*, 1992; *Simpson*, 1994]. This low-level baroclinicity generates mesoscale solenoidal circulation that uplifts moist air within the higher surface temperature region to the condensation level, and on a clear day this may cause a line of clouds to form in an otherwise cloudless sky [*Simpson*, 1994]. This solenoidal circulation has a big impact on weather forecasting, sport sailing, gliding and ballooning, wind farming, sea birds and pest migration, and pollutant distribution [*Simpson*, 1994].

[3] Thermal-gradient-induced cloud-line formation can usually be found near the land/water boundary, where the surface thermal gradient can be large. Documented examples include: along the center axis of lakes, referred to as lake-effect clouds [*Holroyd*, 1971; *Niziol et al.*, 1995] by weather forecasters and glider pilots; in the center of coastal bays [*Sikora et al.*, 2001; *Sikora and Halverson*, 2002]; parallel to the sea/land boundary, known as the sea/land breeze [*Eastwood and Rider*, 1961], in the middle of the Florida peninsula and the Yangtze River where two breeze fronts converge [*Boybeyi and Raman*, 1992; *Yan and Huang*, 1988], and along a major metropolitan street [*Kanda et al.*, 2001]. However, for the open ocean this phenomenon is rarely observed.

[4] In this report we present the satellite observation of a very long cloud line, formed along the Gulf Stream axis. A mesoscale numerical model simulation confirms that the cloud line is formed by the thermal-gradient-induced upward air motion over the center of the Gulf Stream.

2. Satellite Observations

[5] Figure 1a shows a National Oceanic and Atmospheric Administration (NOAA) Advanced Very High Resolution Radiometer (AVHRR) sea surface temperature (SST) image of the waters off the U.S. northeast coast taken at 18:19:41 UTC on April 24, 2001. At the satellite overpass time, the sky is clear over most of the northwest Atlantic. The powerful western boundary current, Gulf Stream characterized by high temperature and salinity, can be clearly seen flowing along the U.S. east coast and leaving the coast after passing Cape Hatteras at approximately 35°N and 75°W. In the middle of the Gulf Stream, a thin cloud line (in white) extends from south of Cape Hatteras toward the northeast at a 36° orientation angle for about 1000 km. Compared to the long length of this cloud line, its width is very narrow (only about 6–7 km). This cloud line matches closely the Gulf Stream's central axis and is about 50 km away from both the Gulf Stream north and south walls which separate the Gulf Stream from the slope water to the west and Sargasso Sea to the east, respectively.

[6] Examining the NOAA/AVHRR SST images taken about two hours before and after Figure 1a, we do not find this cloud line. However, this cloud line is also present in a Sea-viewing Wide Field of view Sensor (SeaWiFS) composite visible false-color image acquired an hour and 17 minutes earlier at 17:02:38 UTC (Figure 1b). This indicates that the lifetime of this phenomenon is only about a few hours. On the SeaWiFS image, the Gulf Stream water is light blue in color, and the cloud line is aligned with the Gulf Stream's axis. Compared to the cloud line width in the later SST image, its width, at about 20–30 km, on the SeaWiFS image is much larger. Therefore, we can deduce that it takes one to two hours for the cloud band to fully converge to the center of the Gulf Stream.

[7] The Gulf Stream cloud line observed in the NOAA/AVHRR SST image is very similar to those observed in the

[1]NOAA National Environmental Satellite, Data, and Information Service, Camp Springs, Maryland, USA.
[2]QSS Group, Inc., Lanham, Maryland, USA.

0094-8276/04/2004GL019892$05.00

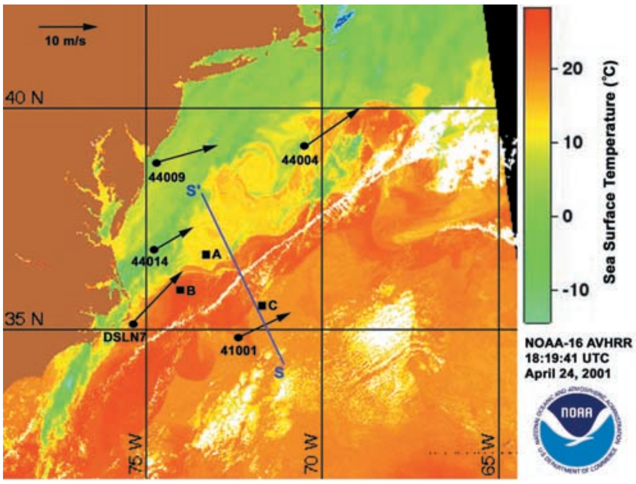

Figure 1a. The NOAA CoastWatch AVHRR SST image from 18:19:41 UTC, April 24, 2001, showing the Gulf Stream and surrounding waters. The Gulf Stream SST is approximately 25.2°C, which is about 7 to 10°C degrees higher than that of the slope and Sargasso Sea waters. A long (1000 km) and thin (6 km) cloud line in white aligns with the major Gulf Stream axis. The surface wind vector measurements (shown in black arrows) by four NOAA moored buoys and a C-MAN station are shown.

middle of the Great Lakes [*Hjelmfelt*, 1990] and the Chesapeake and Delaware Bays [*Sikora et al.*, 2001; *Sikora and Halverson*, 2002]. The favorable conditions for generating this type of "lake-effect" cloud line are a large surface thermal gradient, relatively high synoptic winds on the order of 10 ms^{-1} along the axis of a major lake or bay, a small cross-lake wind component, and a large air-sea temperature difference [*Simpson*, 1994; *Sikora et al.*, 2001]. Conceptually, it is easy to understand why the Gulf Stream will induce this "lake-effect" since its temperature is much higher than that of the surrounding waters.

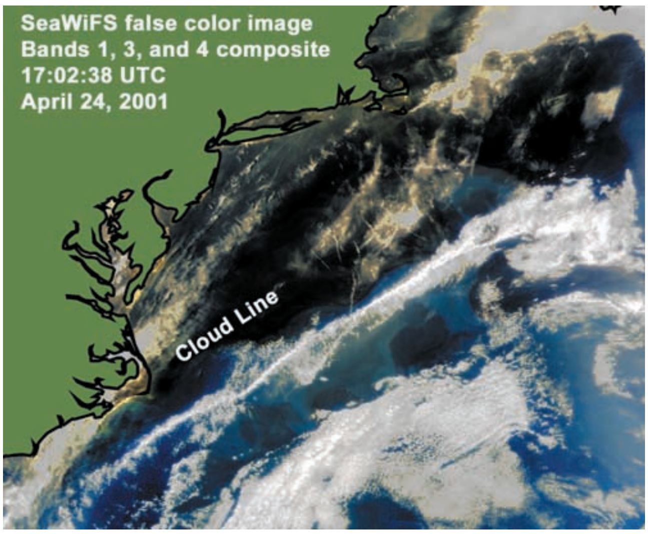

Figure 1b. An OrbView-2 satellite SeaWiFS false color image (composite image of bands 1, 3, and 4) taken at 17:02:38 UTC on April 24, 2001, showing a pronounced visual cloud line (in white) in the middle of the Gulf Stream. The Gulf Stream water is shown in blue.

Table 1. The SST in the Slope Water off the U.S. Northeast Coast, Gulf Stream, and Sargasso Sea Water Measured From NOAA/AVHRR Data

Box A (Slope Water)	Box B (Gulf Stream Water)	Box C (Sargasso Sea Water)
14.3 ± 0.3°C	25.2 ± 0.3°C	18.7 ± 0.3°C

[8] The NOAA/AVHRR SST imagery is processed using the nonlinear split-window algorithm [*Walton et al.*, 1998; *Li et al.*, 2001a] at a spatial pixel resolution of about 1.4 km with an accuracy of 0.5°C [*Li et al.*, 2001b]. The SST values within the Gulf Stream, the Sargasso Sea and the slope waters are each averaged over 500 pixels as indicated by boxes A, B, and C in Figure 1a, and given in Table 1. The Gulf Stream water is approximately 25°C, which is about 10°C and 7°C degrees warmer than that of the slope water and the Sargasso Sea water, respectively. A recent study shows that a temperature gradient of this magnitude may generate a band of clouds covering most of the Gulf Stream and its meanders [*Young and Sikora*, 2003].

3. Surface-Thermal-Gradient-Induced Solenoidal Circulation

[9] Dimensional analysis yields a sea/land solenoidal circulation index [*Simpson*, 1994], $SI = U^2/\Delta T$ where U is the cross-coast wind speed and ΔT is the surface temperature difference. This index represents the balance between the wind and thermal forces which control the establishment of a sea-breeze circulation. A small SI number represents favorable conditions for sea-breeze development. For a larger cross-coast wind speed, the solenoidal circulation may only develop when there is a large surface temperature gradient. The critical SI values, below which the sea-breeze circulation occurs, have been experimentally determined to be between 3 and 10 for different test sites near large lakes and islands [*Biggs and Graves*, 1962; *Lyons and Olsson*, 1972].

[10] For the case examined here, wind measurements, taken about 20 minutes before the NOAA satellite pass by four NOAA moored buoys and one Coastal-Marine Automated Network (C-MAN) station, within the region covered by the satellite SST image are given in Table 2. The surface wind speed is between 6.4 and 10.7 m s^{-1}, and the wind direction is from between 194° and 225° with respect to north. The mean wind from a simple average of these wind measurements is about 9.2 m s^{-1} from 204°. This southwestly wind is moderately strong and is aligned almost parallel to the Gulf Stream's major axis at a similar orientation to that of the cloud line, which is from 216° toward 36°.

Table 2. The Sea Surface Wind Speed and Direction Measured by NOAA Moored Buoys Within the AVHRR SST Image Shown in Figure 1a[a]

Station	Wind Speed (m s^{-1})	Wind Direction From North
44009	9.8	196°
44004	10.3	211°
44014	6.4	194°
DSLN7	10.7	225°
41001	8.8	195°

[a]The wind is measured at 18:00 UTC, about 20 minutes earlier than the NOAA satellite overpass.

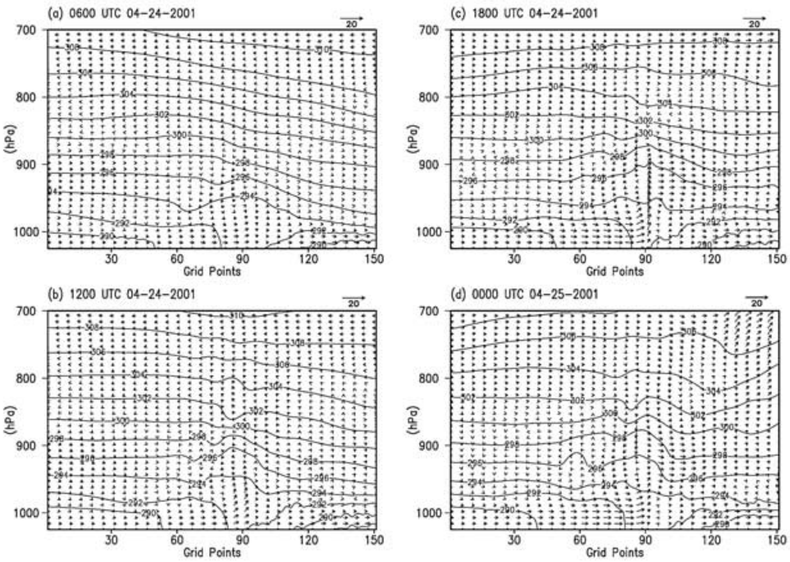

Figure 2. Cross section of vertical circulation (arrows) and potential temperature (contours) through the cloud line indicated in S-S′ in Figure 1. (a) 06 UTC April 24, 2001; (b) 12 UTC same day; (c) 18 UTC same day; (d) 00 UTC April 25, 2001. The arrow to the upper right of each graph shows the scale in m s^{-1} for horizontal velocity and cm s^{-1} for vertical velocity. The contour interval for potential temperature is 2°K.

[11] Using the SST gradient and the cross-Gulf-Stream wind averaged along the Gulf Stream, the estimated *SI* value in this case is about 0.5, which is an order of magnitude smaller than the *SI* critical value. In any case, this *SI* value is very favorable for sea-breeze-like solenoidal circulation to occur.

[12] If the synoptic wind component perpendicular to the Gulf Stream's axis becomes stronger, then the *SI* value increases by the square of the wind speed, destroying the mesoscale solenoidal circulation [*Sikora et al.*, 2001]. The cross wind blows away the heat and moisture necessary for setting up the system. The critical wind angle with respect to the major axis of the heating source, α, is a function of regional temperature, temperature gradient, air-sea temperature difference, wind speed and direction and width of the heating source. It is defined as [*Sikora et al.*, 2001]: $\alpha = \arcsin(\sqrt{1.59gWC_H(T_{sea} - T_{air})/TU^2})$ where g is the acceleration of gravity; W is the width of the heating source; C_H is the bulk heating transfer coefficient with a value of 1.1×10^{-3}; T_{sea}, T_{air}, and T are sea, air and regional averaged temperatures in K, respectively. The favorable solenoidal circulation condition is reached when the angle between the wind vector and the major axis of the heating source is less than α. The width of the Gulf Stream (heating source) is 100 km, the averaged SST is 20°C, and $T_{sea} - T_{air}$ = 4°C. For this set of environmental conditions, the calculated α is about 32°. The actual observed angle between the Gulf Stream's major axis and the synoptic wind vector is 12° (216° − 204° = 12°), which is well below the critical minimum wind angle.

4. Numerical Simulation of Low-Level Atmospheric Circulation Over the Gulf Stream

[13] The fifth-generation Pennsylvania State University (PSU)-National Center for Atmospheric Research (NCAR) Mesoscale Model version 5 (MM5) [*Grell et al.*, 1995], is used to simulate the low-level atmospheric circulation for the Gulf Stream region on April 24, 2001. The fundamental model features used in this study include (i) the Blackadar planetary boundary layer scheme [*Zhang and Anthes*, 1982], (ii) the simultaneous use of the new version of the Kain-Fritsch [*Kain and Fritsch*, 1993] convective parameterization including the parameterizated shallow convective effects [*Deng et al.*, 2003] and a simple explicit treatment of cloud microphysics based on [*Dudhia*, 1989], (iii) a simple radiative cooling scheme, (iv) a multilayer soil model to predict land surface temperatures by using the surface energy budget equation, and (v) the specification of the outermost coarse-mesh lateral boundary conditions by linearly interpolating National Centers for Environment Prediction (NCEP) 3-hourly Eta Model analyses at the resolution of 40 km on the Advanced Weather Interactive Processing System 212 grid.

[14] A two-way, nested-grid (27/9 km) technique is employed to achieve a multi-scale simulation. The coarse domain, centered at 37.5°N and 72.5°W, covers the region approximately 29.5°–44.5°N and 82°–63°W and the fine domain covers the region approximately 33.5°–40.3°N and 77°–67°W. A total of 31 σ levels in the vertical direction are used, with the model top at 50 hPa. These full σ levels are 0.0, 0.04, 0.08, 0.12, 0.16, 0.20, 0.24, 0.28, 0.32, 0.36, 0.40, 0.44, 0.48, 0.52, 0.56, 0.60, 0.64, 0.68, 0.72, 0.76, 0.80, 0.84, 0.87, 0.90, 0.92, 0.938, 0.956, 0.97, 0.982, 0.992, and 1, which give 30 half-σ layers. The model is initiated at 0000 UTC April 24, 2001 and then integrates continuously for 24 hours. The initial and boundary conditions are defined with NCEP's Eta Model analyses.

[15] Figure 2 shows the horizontal and vertical velocities along the S-S′ transect indicated in Figure 1a at 6-hr intervals on April 24, 2001. Since the synoptic wind is roughly parallel to the Gulf Stream axis, the horizontal component is obviously small. At the lower atmospheric levels between the 294°K and 296°K potential temperature

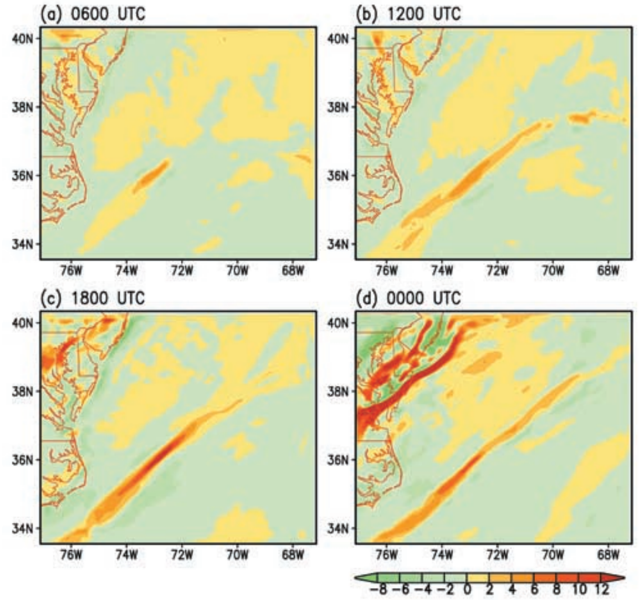

Figure 3. Distribution of vertical velocity fields (cm s^{-1}) at 950 hPa at 06 UTC (a), 12 UTC (b), 18 UTC (c) on April 24, 2001, and 00 UTC on April 25, 2001 (d).

contour lines, the time series plots show the increase of vertical motion from almost 0 cms^{-1} at 06 UTC April 24 to its strongest at 12 cms^{-1} at 18 UTC and then its subsequent decrease to about 2–3 cms^{-1} at 00 UTC on April 25. The height of the solenoidal circulation reaches to about the 900 hPa level at 18 UTC. The corresponding 296°K potential temperature line rises and falls with the strength of this upward motion. We further examine the horizontal distribution of the vertical motion that is associated with the cloud-line formation. Figure 3 shows the time series of the distribution of vertical velocity distribution at the 950 hPa level in the model domain. The upward motion at this level reaches its maximum at 18 UTC and the center of the upward motion is collocated with the Gulf Stream center axis and matches the cloud line pattern; thus, this model-revealed dynamical process agrees well with satellite observations.

5. Conclusions

[16] In this study, we present satellite observations of a very long (1000 km) cloud line aligned with the Gulf Stream axis. From wind and surface temperature analyses, we determined that the environmental conditions were favorable for generating the mesoscale solenoidal circulation observed in the two satellite images. The Gulf Stream cloud line resembles a "lake-effect" cloud line, frequently observed in the middle of large lakes, but with a much larger scale. This large-scale cloud-line phenomenon is rarely observed in the ocean, even in areas of high surface thermal gradient, mainly because large surface-thermal-gradient regions such as the Gulf Stream and other major high-temperature, western boundary currents are also areas with high cloud coverage. Moderate-to-strong wind parallel to the Gulf Stream, and clear sky conditions rarely happen coincidently.

[17] Although similar cloud-line formations can be generated by other mechanisms, i.e., airplane or missile trails and ship tracks [*Coakley et al.*, 1987; *Rakde et al.*, 1989; *Conover*, 1966], we dismiss these possibilities because this cloud line does not disperse, but actually continues to converge between the time of the two satellite images, and neither does it show significant differences from one end to the other.

[18] **Acknowledgments.** We acknowledge support from the NOAA Ocean Remote Sensing Program. The SeaWiFS image in Figure 1b is provided by the SeaWiFS Project, NASA/Goddard Space Flight Center. We would like to thank Eric Bayler and Alan Strong for their valuable inputs during the internal review process and two anonymous reviewers for their helpful comments. The views, opinions, and findings contained in this report are those of the authors and should not be construed as an official National Oceanic and Atmospheric Administration or U.S. Government position, policy, or decision.

References

Biggs, W. G., and M. E. Graves (1962), A lave breeze index, *J. Appl. Meteorol.*, *1*, 474–480.
Boybeyi, Z., and S. Raman (1992), A three-dimensional numberical sensitivity study of convection over the Florida peninsula, *Boundary Layer Meteorol.*, *60*, 325–359.
Coakley, J. A., Jr., R. L. Bernstein, and P. A. Durkee (1987), Effect of ship-stack effluents on cloud reflectivity, *Science*, *237*, 1020–1022.
Conover, J. H. (1966), Anomalous cloud lines, *J. Atmos. Sci.*, *23*, 778–785.
Deng, A., N. L. Seaman, and J. S. Kain (2003), A shallow-convective parameterization for mesoscale models, part I: Submodel description and preliminary application, *J. Atmos. Sci.*, *60*, 34–56.
Dudhia, J. (1989), Numerical study of convection observed during the winter monsoon experiments using a mesoscale two-dimensional model, *J. Atmos. Sci.*, *46*, 3077–3107.
Eastwood, E., and G. C. Rider (1961), A radar observation of a sea breeze front, *Nature*, *189*, 978–990.
Grell, G. A., J. Dudhia, and D. R. Stauffer (1995), A description of the fifth-generation Penn State/NCAR Mesoscale Model (MM%), *NCAR Tech. Note NCAR/TN-398+STR*, 122 pp., Natl. Cent. for Atmos. Res., Boulder, Colo.
Hjelmfelt, M. R. (1990), Numerical study of the influence of environmental conditions on lake-effect snowstorms over Lake Michigan, *Mon. Weather Rev.*, *118*, 138–150.
Holroyd, E. W. (1971), Lake-effect cloud bands as seen from weather satellites, *J. Atmos. Sci.*, *28*, 1165–1170.
Holton, J. R. (1992), *An Introduction to Dynamic Meteorology*, Academic, San Diego, Calif.
Kain, J. S., and J. M. Fritsch (1993), Convective parameterization for mesoscale models: The Kain-Fritsch scheme—The representation of cumulus convection in the numerical models, *Meteorol. Monogr.*, *46*, 165–170.
Kanda, M., Y. Inoue, and I. Uno (2001), Numerical study on cloud lines over and urban street in Tokyo, *Boundary Layer Meteorol.*, *98*, 251–273.
Li, X., W. Pichel, E. Maturi, P. Clemente-Colón, V. Krasnopolsky, and J. Sapper (2001a), Deriving the operational nonlinear multi-channel sea surface temperature algorithm coefficients for NOAA-15 AVHRR/3, *Int. J. Remote Sens.*, *22*, 699–704.
Li, X., W. Pichel, P. Clemente-Colón, V. Krasnopolsky, and J. Sapper (2001b), Validation of coastal sea and lake surface temperature measurements derived from NOAA/AVHRR data, *Int. J. Remote Sens.*, *22*, 1285–1303.
Lyons, W. A., and L. E. Olsson (1972), The climatology and prediction of the Chicago lake breeze, *J. Appl. Meteorol.*, *11*, 1254–1272.
Niziol, T. A., W. R. Snyder, and J. S. Waldstreicher (1995), Winter weather forecasting throughout the eastern United States. Part IV: Lake effect snow, *Weather Forecasting*, *10*, 61–76.
Rakde, L. F., Jr., J. A. Coakley, and M. D. King (1989), Direct and remote sensing observations of the effect of ships on clouds, *Science*, *246*, 1146–1149.
Sikora, T. D., and D. M. Halverson (2002), Multiyear observations of cloud lines associated with the Chesapeake and Delaware Bays, *J. Appl. Meteorol.*, *41*, 825–831.
Sikora, T. D., G. S. Young, E. E. O'Marr, and R. F. Gasparovic (2001), Anomalous cloud lines over the mid-Atlantic coast of the United States, *Can. J. Remote Sens.*, *27*, 320–327.
Simpson, J. E. (1994), *Sea Breeze and Local Winds*, Cambridge Univ. Press, New York.

Walton, C. C., W. G. Pichel, J. F. Sapper, and D. A. May (1998), The development and operational application of nonlinear algorithms for the measurement of sea surface temperatures with the NOAA polar-orbiting environmental satellites, *J. Geophys. Res.*, *103*, 27,999–28,012.

Yan, B., and R. Huang (1988), A numerical study of the land and river breezes over Chongqing on the Yangtze River, *Chin. J. Atmos. Sci.*, *13*, 159–170.

Young, G. S., and T. D. Sikora (2003), Mesoscale stratocumulus bands caused by Gulf Stream meanders, *Mon. Weather Rev.*, *131*, 2177–2191.

Zhang, D.-L., and R. A. Anthes (1982), A high-resolution model of the planetary boundary layer—Sensitivity tests and comparisons with SESAME-79 data, *J. Appl. Meteorol.*, *21*, 1594–1609.

P. Clemente-Colón, K. S. Friedman, X. Li, W. G. Pichel, and C.-Z. Zou, NOAA/NESDIS, E/RA3, Rm 102, 5200 Auth Road, Camp Springs, MD 20746, USA. (xiaofeng.li@noaa.gov)

W. Zheng, QSS Group, Inc., 4501 Forbes Blvd, #200, Lanham, MD 20706, USA.